Electronic Supplementary Material (ESI) for Green Chemistry.

Electronic Supplementary Information

Free-standing $LiFePO_4$-carbon paper hybrid cathode for flexible Lithium-ion batteries

Katja Kretschmer, Bing Sun*, Xiuqiang Xie, Shuangqiang Chen and Guoxiu Wang*

Centre for Clean Energy Technology, School of Mathematics and Physical Sciences, University of Technology Sydney, Sydney NSW 2007, Australia.

Bing.sun@uts.edu.au , Guoxiu.Wang@uts.edu.au

Table 1: GEM Commodity prices of wood pulp and aluminium from 2010 to 2014.[1]

	2010	2011	2012	2013	2014
Wood pulp [US$/t]	866.79	899.65	762.84	823.08	876.91
Aluminium [US$/t]	2173.12	2401.39	2023.28	1846.67	1867.42

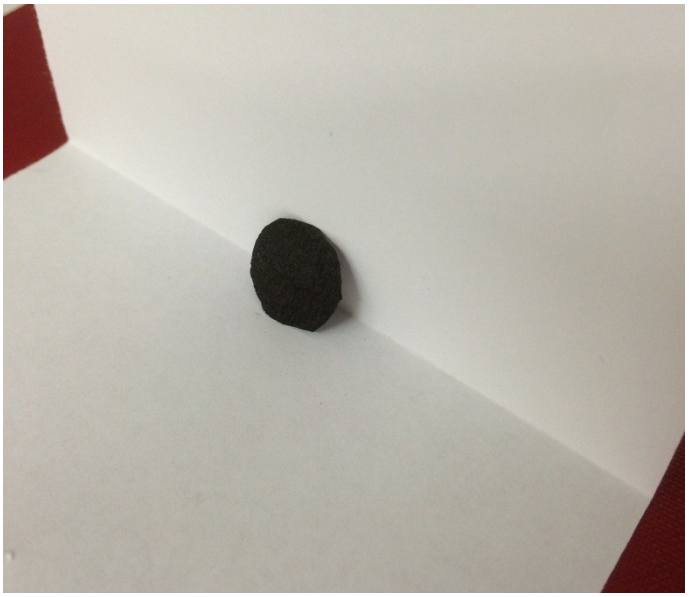

Figure S1: Digital photograph of the free-standing $LiFePO_4$@CP hybrid electrode.

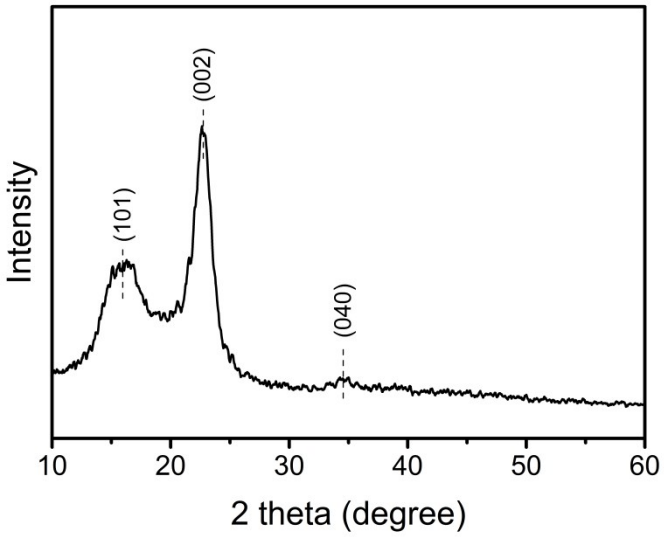

Figure S2: Measured XRD pattern of purified paper towel matching the standard XRD pattern of microcrystalline cellulose.[2-3]

Electrode preparation process: For the impregnation with solution 1 (STEP 1 in Scheme 1 main article) consisting of the phosphate and lithium precursor salts, it is important to understand the precipitation mechanism of $LiOH{\cdot}H_2O$ and $NH_4H_2PO_4$ and the subsequent acid-assisted dissolution of Li_3PO_4. This allows validating the weight gain as an accurate marker to calculate the amount of solution 2, which contains the iron and carbon precursors, needed to generate the correct stoichiometric ratio of $LiFePO_4$ impregnated into the PT network. The first reaction between the two precursor materials is the precipitation of Li_3PO_4, wherein all Li ions are consumed (1). The residual $NH_4H_2PO_4$ dissolves to form aqueous phosphoric acid (H_3PO_4) and NH_3 (2). Hydrochloric acid (HCl) then dissolves the Li_3PO_4 precipitate to form LiCl and LiH_2PO_4 (3), wherein LiCl is consumed by H_3PO_4 to form crystalline LiH_2PO_4 upon solvent and HCl evaporation (4).[4] Consequently, the freeze-drying process leaves the PT impregnated with highly crystalline LiH_2PO_4 homogenously dispersed throughout the fibre network.

$$3LiOH \cdot H_2O + NH_4H_2PO_4 \rightarrow Li_3PO_4(s) + NH_3 + 6H_2O \quad (1)$$

$$NH_4H_2PO_4 \rightarrow H_3PO_4 + NH_3 \quad (2)$$

$$Li_3PO_4 + 2HCl \rightarrow 2LiCl + LiH_2PO_4 \quad (3)$$

$$LiCl + H_3PO_4 \rightarrow LiH_2PO_4 + HCl \quad (4)$$

The reaction mechanism in solution 1 as described in equation (1) to (4) has been confirmed by the XRD pattern of the dried solution (Figure S3). The traces of LiCl are negligible due to the pure phase XRD pattern of the final product (Figure 1 main article). It can be assumed that this minor Li excess does not result in the formation of impurities, such as Li_3PO_4.[5-6] On the contrary, a slight oversupply of lithium during solid-state preparation methods is considered beneficial to compensate for the loss of the lithium element caused by the evaporation of Li_2O.[7] These residual LiCl crystals are possibly caused by an undersupply of phosphoric acid (H_3PO_4). According to the theoretical assumption of the reaction mechanism during freeze-drying of solution 1, the mass of the $Fe(III)Cl_3$ solution (solution 2) needed to ensure the appropriate molar ratio $Li:Fe:PO_4=1:1:1$ can be sufficiently calculated from the mass load of PT. The impregnation of the iron precursor (STEP 2 in Scheme 1 main article) includes the dissolved carbon precursor, which is applied as reducing agent and to generate a conductive carbon coating on the surface of the $LiFePO_4$ layer, which also serves as structural support. The next stage of the electrode preparation is the two-stage heat treatment (STEP 3 in Scheme 1 main article). The first heat treatment stage at 312 °C was chosen to allow $Fe(III)Cl_3$ to melt and consequently enable capillary forces to homogenously distribute it through the PT fibre network. The decomposition of all precursor materials, the

crystal formation of $LiFePO_4$, and the carbon network generation takes simultaneously place in the second and final heat treatment stage from 312 °C to 700 °C.

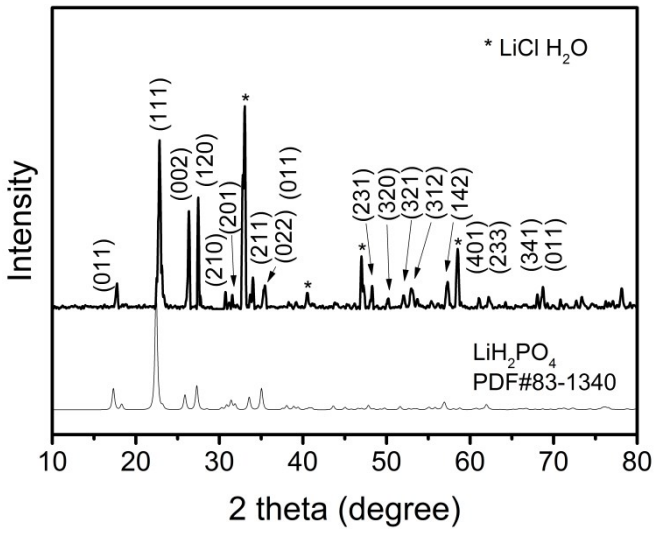

Figure S3: XRD pattern of solution 1 after drying compared with the simulated pattern of LiH_2PO_4 calculated from JCPDS card number 83-1340 (* marks traces for $LiCl{\cdot}H_2O$).

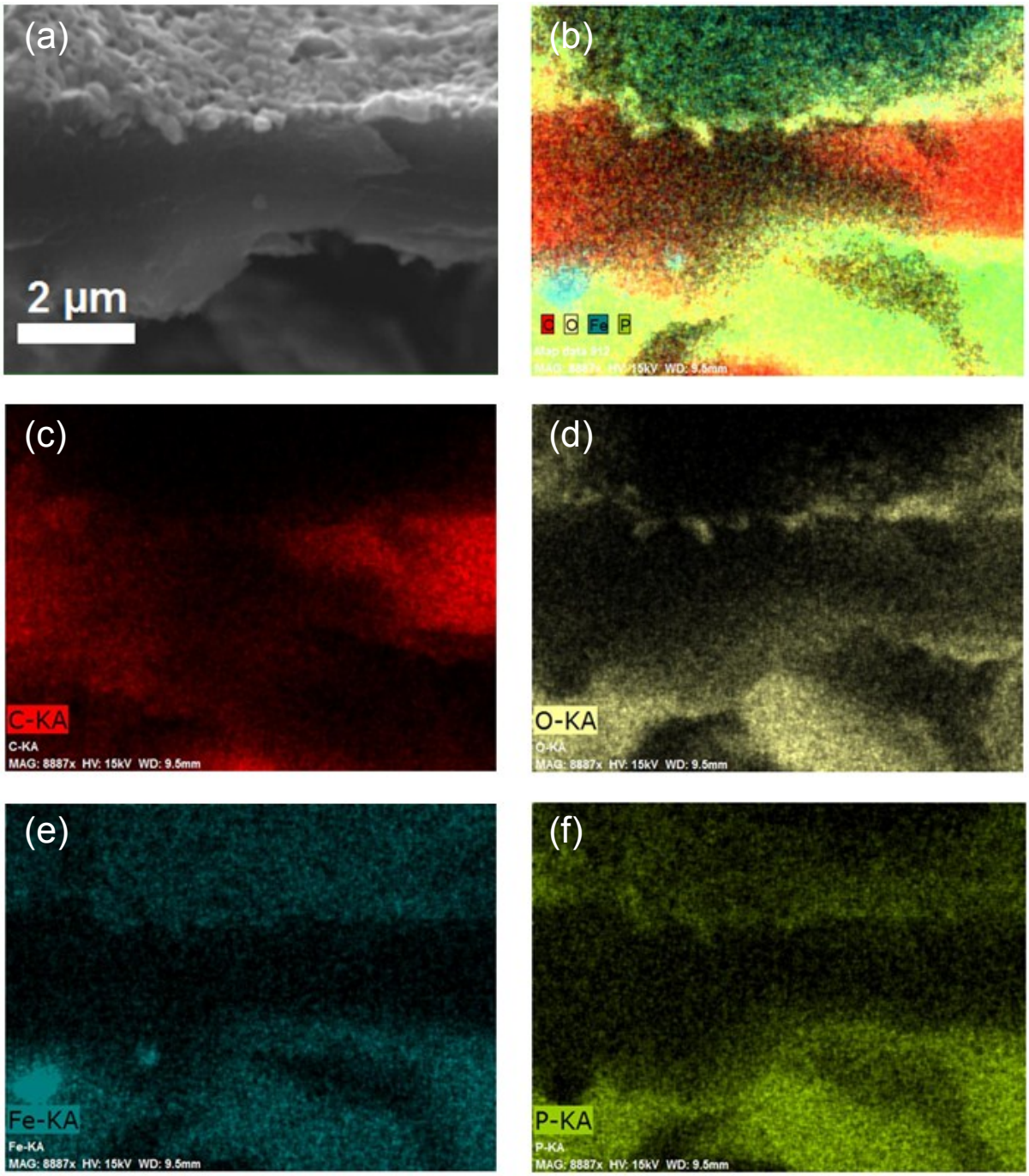

Figure S4: SEM energy-dispersive spectroscopy (EDS) characterization of $LiFePO_4$@CP. (a) SEM image of the selected area for EDS mapping; (b) Integrated Fe-, P-, O-, and C-elemental mapping image; elemental mapping images of (c) carbon C, (d) oxygen O, (e) iron Fe, and (f) phosphorous P.

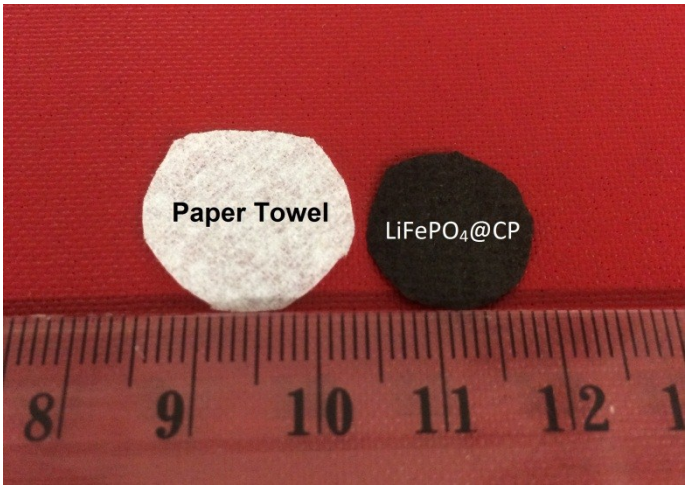

Figure S5: Digital photograph to visualize the shrinkage of the cellulose substrate (paper towel) to $LiFePO_4$@C after carbonization.

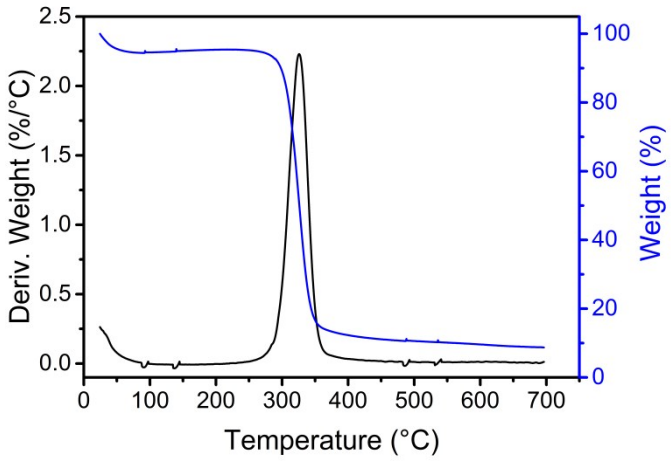

Figure S6: TGA/DTA analysis of PT carbonized in the temperature range from room temperature to 700 °C under nitrogen flow with a heating rate of 5 °C min^{-1}

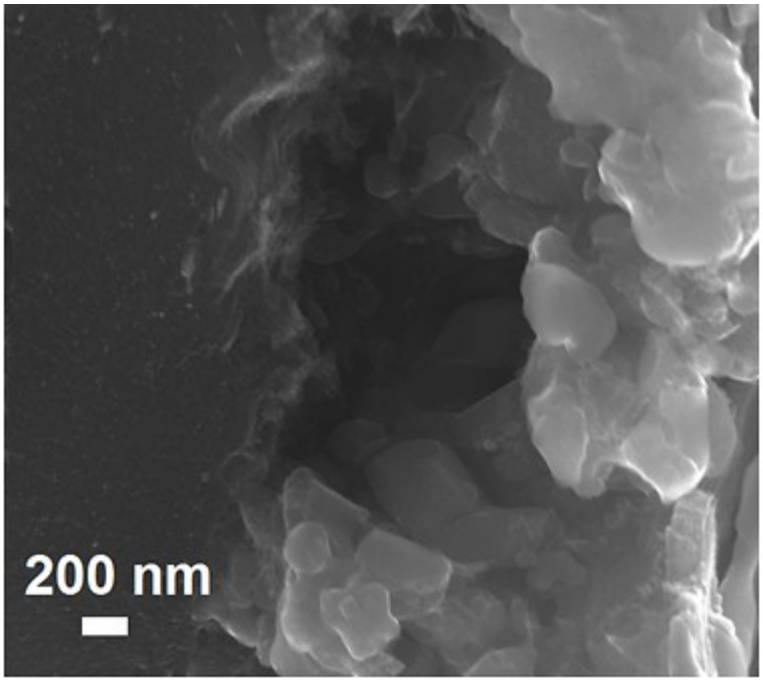

Figure S7: High magnification SEM of $LiFePO_4$@CP showing a cavity inside the dense shell

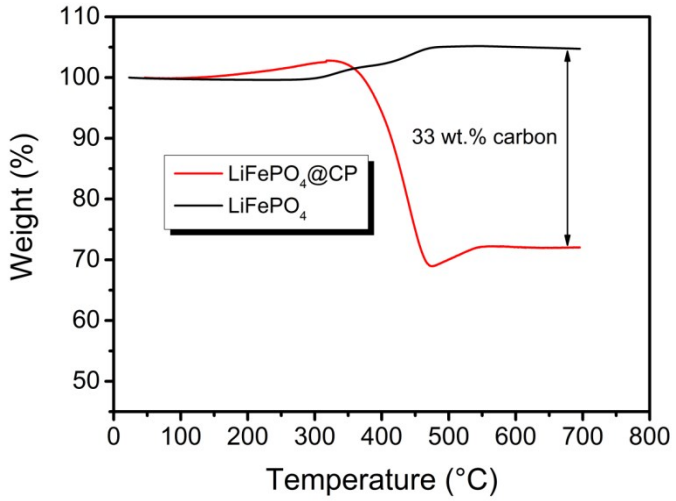

Figure S8: TGA curve of $LiFePO_4$@CP and carbon free $LiFePO_4$ from room temperature to 700 °C in air

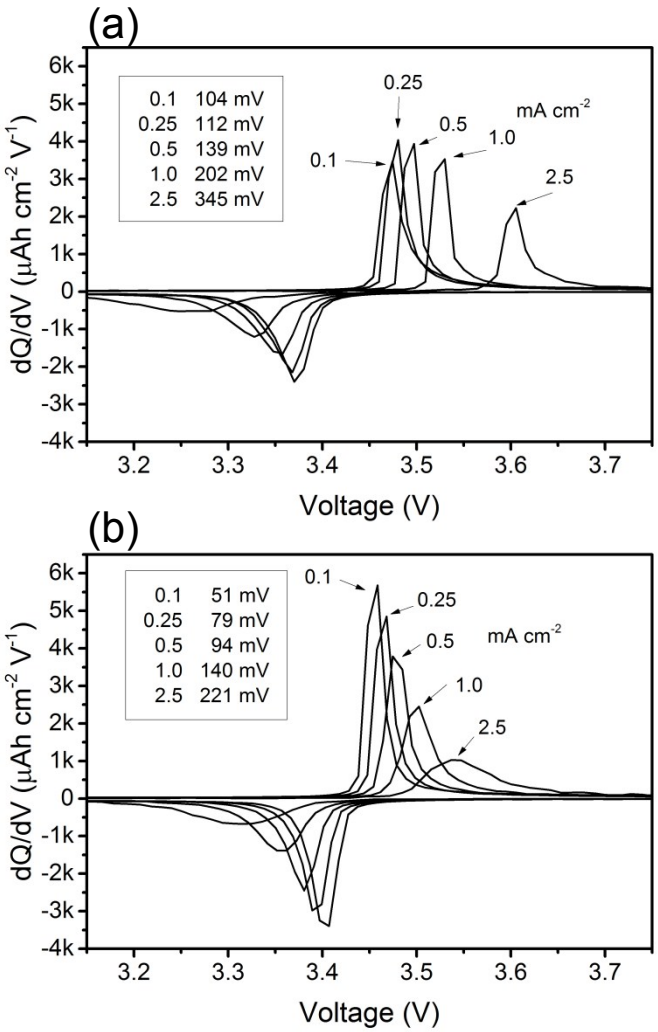

Figure S9: Corresponding differential capacity analysis of (a) step one and (b) step three of $LiFePO_4$@CP (Insets: Overpotentials in mV for the current densities 0.1 to 2.5 mA cm^{-2})

Preparation of $LiFePO_4$ cathode materials: $LiFePO_4$ was prepared by mixing stoichiometric amounts of $FeC_2O_4{\cdot}2H_2O$, $NH_4H_2PO_4$ and Li_2CO_3 (Sigma-Aldrich) *via* industrial-scale ball milling in deionized water for 6 h. Simultaneously, 5 wt.% sucrose was added to the suspension to encapsulate the precursor materials during spray drying and to serve as a carbon source in the subsequent carbothermal reduction. The solid content of the suspension was fixed at 20 wt.%. The untreated precursor mixture was spray-dried (Mini Spray Dryer B290, BÜCHI Labortechnik AG, Switzerland) with an inlet temperature of 170 °C and a feed rate of 15 ml min^{-1}. The dried power was then transferred into a ceramic crucible to thermally decompose in a tubular furnace at 350 °C for 5 h and sintered at 700 °C for 10 h under argon protection. The working electrodes of $LiFePO_4$@Al for electrochemical testing were prepared by mixing 80 wt.% as-prepared $LiFePO_4$ with 10 wt.% carbon black and 10 wt.% poly(vinyl difluoride) (PVDF, Sigma-Aldrich) in N-Methyl-2-pyrrolidone (NMP, Sigma-Aldrich). The obtained dispersion was carefully pasted onto aluminium foil, dried in a vacuum at 80 °C for 12 h and pressed before cell assembly. The cell assembly was conducted as described in the experimental section.

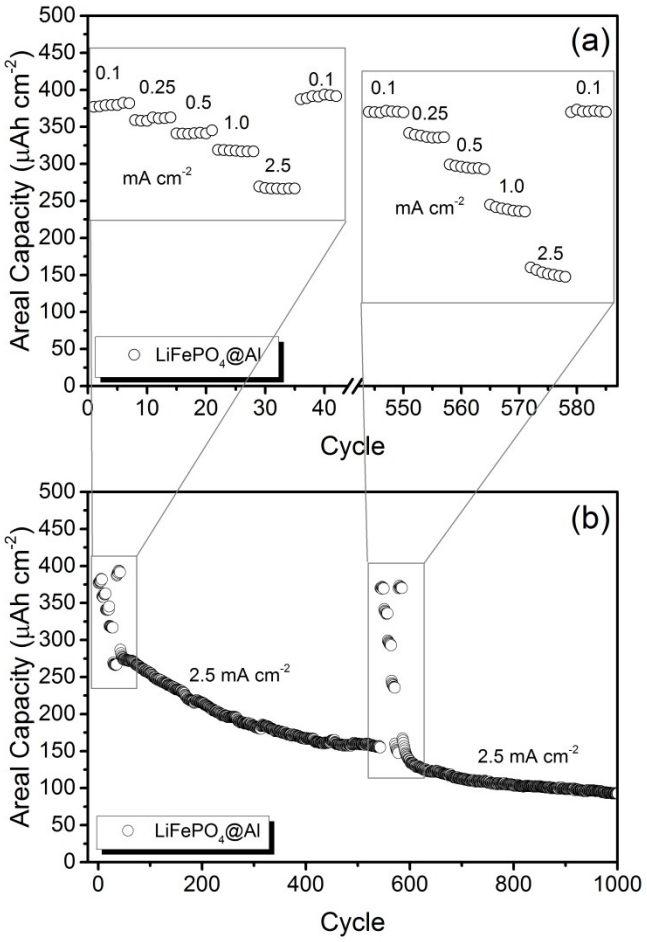

Figure S10: (a) Rate performance and (b) stability test sequence of a traditional $LiFePO_4$@Al displayed in areal capacity. The active material mass load of all electrodes is around 2.8 mg cm^{-2}.

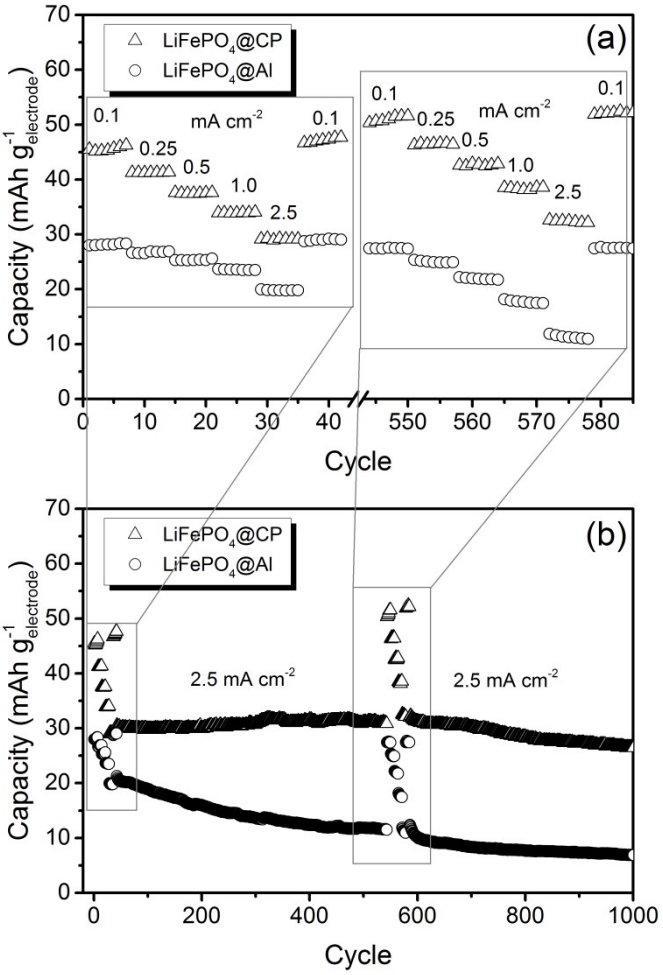

Figure S11: (a) Rate performance and (b) stability test sequence of $LiFePO_4$@CP and a traditional $LiFePO_4$@Al. The capacity is displayed in mAh per gram of electrode (weight including current collector, binder and additives). The active material mass load of all electrodes is around 2.8 mg cm^{-2}.

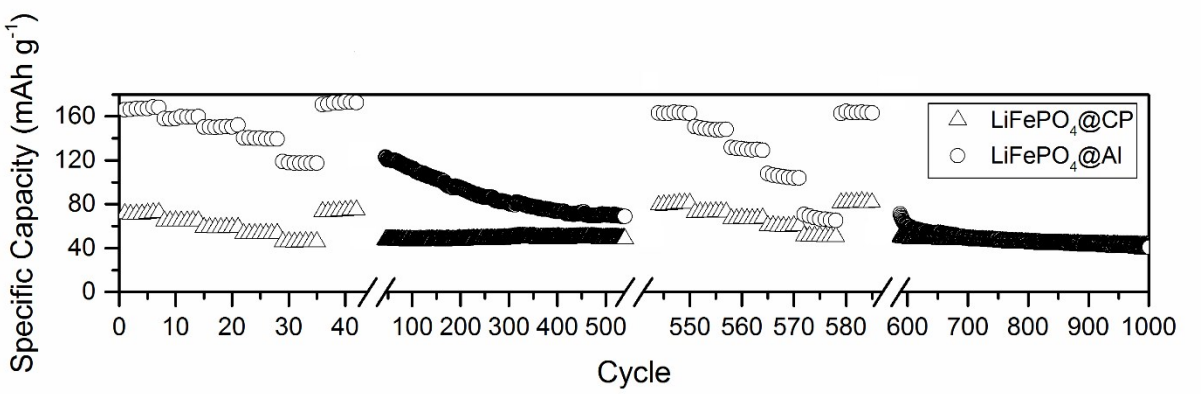

Figure S12: Rate performance and stability test sequence of $LiFePO_4$@CP and a traditional $LiFePO_4$@Al. The capacity is displayed in mAh per gram active material. The active material mass load of all electrodes is around 2.8 mg cm^{-2}.

References

[1] http://data.worldbank.org/data-catalog/commodity-price-data, The World Bank Group, **2015**.

[2] X. Ju, M. Bowden, E. E. Brown, X. Zhang, *Carbohydrate Polymers* **2015**, *123*, 476–481.

[3] Q. Pang, L. Wang, H. Yang, L. Jia, X. Pan, C. Qiu, *RSC Advances* **2014**, *4*, 41212-41218.

[4] A. P. Voronov, G. N. Babenko, V. M. Puzikov, A. N. Iurchenko, *Journal of Crystal Growth* **2013**, *374*, 49-52.

[5] G. X. Wang, H. Liu, J. Liu, S. Qiao, G. M. Lu, P. Munroe, H. Ahn, *Advanced Materials* **2010**, *22*, 4944-4948.

[6] B. Kang, G. Ceder, *Nature* **2009**, *458*, 190-193.

[7] L. Yang, G. Liang, L. Wang, X. Zhi, X. Ou, *Journal of Alloys and Compounds* **2010**, *496*, 376-379.